Stress and strain dependent stiffness in a numerical model of a tunnel

J. Boháč
Charles University, Prague, Czech Republic

I. Herle
Academy of Sciences, Prague, Czech Republic

D. Mašín
Charles University, Prague, Czech Republic

ABSTRACT: In the current road tunneling project in the centre of Prague, Czech Republic, several tectonic faults were encountered. The joints are filled by fragments of shales in a silty to clayey matrix. In the laboratory, the behaviour of the material was studied using mixtures of sand or crushed rock with fines at different mixing ratios. Further laboratory tests were carried out with the material from the joints, both on reconstituted and undisturbed triaxial specimens. The laboratory data are used in the numerical simulation of deformations of the rock massif during the tunnel construction. A comparison of several constitutive models for the fault material is presented, from a linear-elastic perfectly-plastic model to a stress and strain dependent stiffness model, and advantages of the stress and strain dependent model are demonstrated.

1 INTRODUCTION

Additional exploitation of urban areas is often possible only by underground structures. However, deformations during the construction of tunnels are inevitable and their impact on buildings must be taken into account. Consequently, there is an increasing need for realistic calculations of surface settlements induced by the construction of shallow tunnels. Semiempirical approaches of the settlement (e.g., Mair et al, 1993) are usually linked to specific soil and/or rock types and may be of little benefit in other geological conditions. Then a numerical (FE) analysis remains the only tool which can help in assessing expected deformations.

Mrázovka tunnel in Prague is designed as a part of the city highway system. The subsoil of the large diameter, two to three-lane twin tunnels, consists mainly of clayey and silty shales of different age and weathering degree. The depth of the overburden varies from 15 to 40 metres. However, in the most critical stretch, under heavily developed urban environment the typical overburden is about 20 m. The geological site investigation revealed that weak zones (tectonic faults - joints) intersect the tunnel profile at several locations (Chmelař and Vorel, 2000).

The aim of the present paper is to show the influence of the joints on the predicted settlement. Since the properties of the filling of the joints were expected to play an important role, an extensive laboratory investigation preceeded the numerical analysis.

2 LABORATORY EXPERIMENTS

The filling of the joints consists of angular fragments of the rock, ranging from a few millimetres up to a few hundred millimetres, in a silty to clayey matrix (Figure 1). Laboratory tests were carried out on the material from the joints, as well as on a model material prepared in the laboratory by mixing coarse-grained and fine-grained soils at different mixing ratios (Mašín, 2001).

1.1 *Tests on fragments within fine-grained matrix*

Two types of coarse-grained admixture were used in the study, an alluvial sand or crushed rock, both having grains larger than 0.125 mm. They were used to model the influence of spherical and angular coarse-grained particles, respectively. A clayey soil with a content of
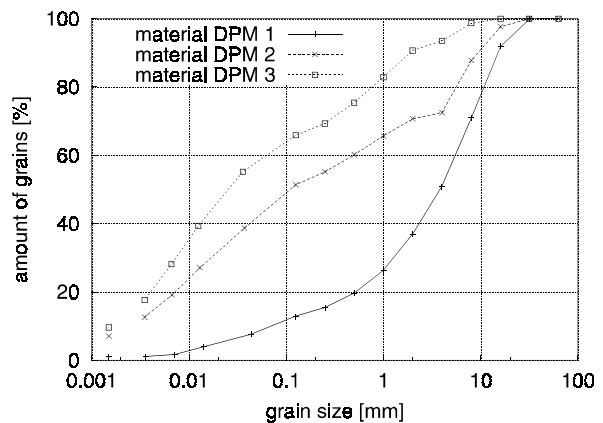

Figure 1. Grading curves of the filling of three tectonic faults DPM1, DPM2 and DPM3.
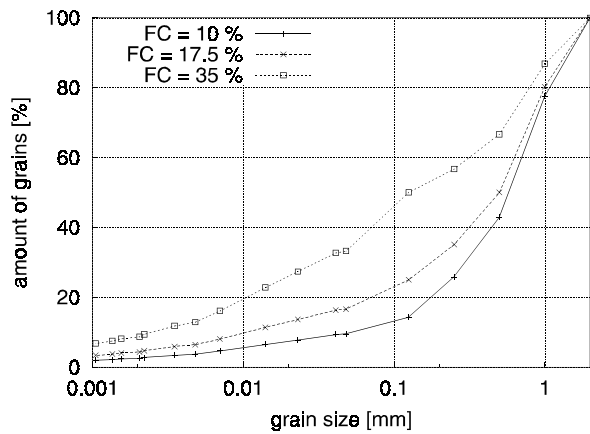
Figure 2. Grading curves of tested model mixtures of clayey soil and crushed rock.

Figure 3. Voids ratios of consolidated triaxial specimens and transition voids ratios.

fines FC (clay and silt particles, i.e., particles smaller than 0.063 mm) of about 70 % was used as the second constituent. An example of the particle size distribution of tested mixtures is in Figure 2.

The mixtures may be expected to behave as a coarse-grained constituent itself if the voids ratio of the coarse-grained fraction e_s is less than its maximum voids ratio $e_{s,max}$. On the contrary, when the voids ratio $e_s > e_{s,max}$ the mixture may behave as a fine-grained soil. From this simple assumption a transition voids ratio and/or transition FC can be estimated (e.g., Thevanayagam and Mohan, 2000).

Voids ratios of triaxial specimens after consolidation, for both spherical and angular grains, are plotted against the content of fines FC in Figure 3. The lines corresponding to the maximum density of the two coarse-grained fractions are also shown. The transition FC can be roughly estimated as 15% and 25% for sand and crushed rock admixture, respectively.

Data in Figure 4 suggest that the transition zone with respect to FC corresponds reasonably well in the case of the critical state strength. The peak strength seems to be influenced even by a very small admixture of fines, the friction angle dropping gradually in a
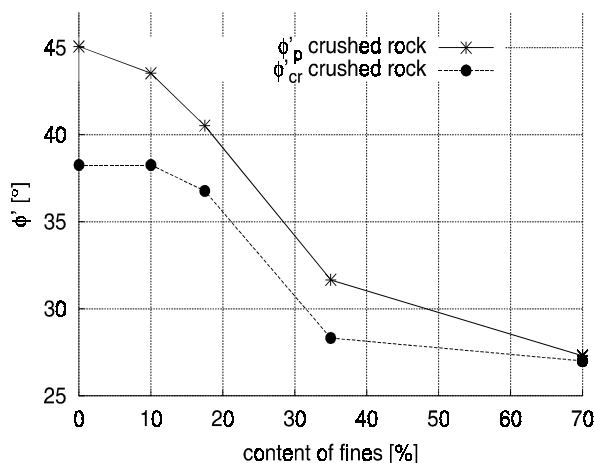
much broader interval of FC. Generally, in the critical state the mixtures seemed to comply with the simple structural theory reasonably well. The peak parameters, on the other hand, changed even after a small percentage of fines was added. It is suggested that the small amounts of fines were sufficient to influence the structure of the laboratory specimens by acting in the contacts of sand-sized grains, and therefore decreasing the shear resistance and/or other quantities. Only after a substantial shearing, when approaching the critical state, the fines were moved from the grains' contacts into the pores of the low FC specimens.

This mechanism is also believed to explain the influence of fines on Young's modulus E of the triaxial specimens shown in Figure 5. The moduli of the specimens with FC 10% and 17.5% are almost equal, being lower than E of crushed rock without fines. Apparently even at such small FC there was no direct contact between coarse-grained particles. The soil behaviour was however influenced by the coarse-grained skeleton which still increased Young's modulus. The role of the coarse-grained skeleton was also manifested by the dilatant behaviour of the specimens. This influence vanished only at the FC of 35%.
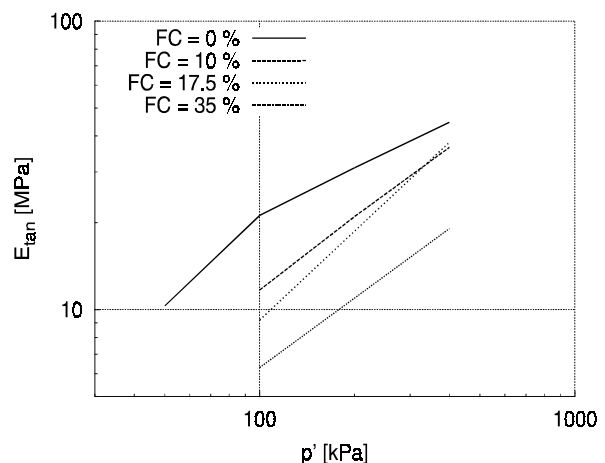

Figure 4. Strength of mixtures of crushed rock with respect to FC.

Figure 5. Dependence of the stiffness of different mixtures of crushed rock on the stress level.
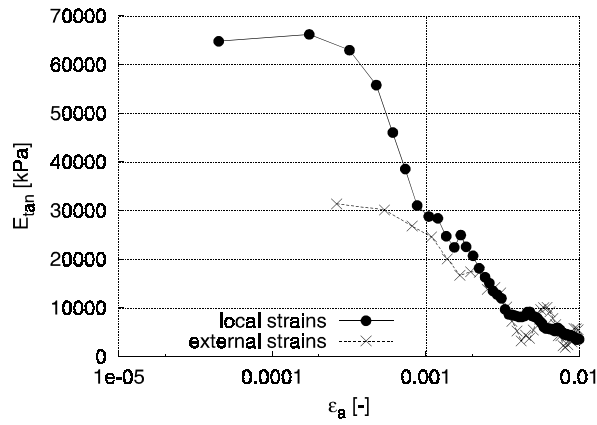
Figure 6. Tangent Young's modulus of filling DPM3.

Figure 7. Strength of filling measured with and without fraction > 4 mm.

1.2 *Samples from the joints*

The particle size distribution of the filling from the three weak zones that were studied by laboratory tests is in Figure 1. In preparing reconstituted triaxial specimens of the diameter of 38 mm, particles larger than 4 mm were removed.

Further to the standard triaxial instrumentation, local axial LVDTs of the resolution of 10^{-4} mm were used in testing the small strain stiffness on two undisturbed specimens of the material DPM3. The comparison of the tangent Young's modulus measured using standard external and local gauges is presented in Figure 6. In this case the stiffness measured by local axial gauges is about twice the stiffness from external measurements.

Further to the triaxial testing on 38 mm diameter specimens, the rock material was also tested in a large diameter shear box of the cross section of 1 m × 1 m. This enabled rock fragments of up to 150 mm to be included in the reconstituted specimens. Therefore the strength measured on the original filling material could be compared with the results from the specimens with particles smaller then 4 mm that were tested in the triaxial apparatus.

Tests on the specimens without gravel and cobble-sized fragments yielded practically the same
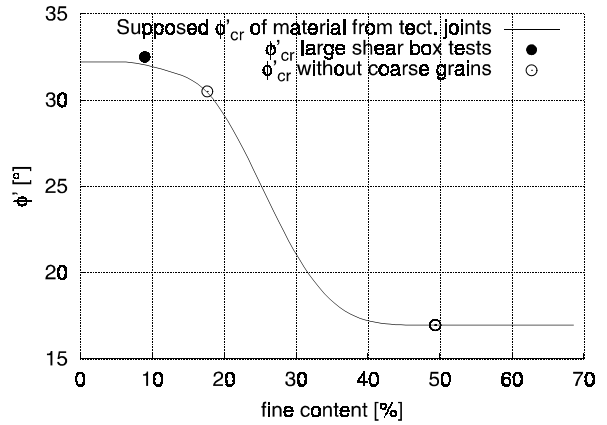
friction angle as tests on the specimens of the original particle size distribution (Figure 7), provided the content of fines FC was the same in both samples. Generally, since a simple removal of coarse fraction changes FC of the soil, the material must be treated prior testing to maintain the original FC. However, the tests on mixtures proved that removal of coarse fragments did not have any influence on the friction angle for specimens above the transition FC.

2 COMPUTATION OF SETTLEMENTS

2.1 *Numerical model*

Although the non-linearity of the soil and rock behaviour is obvious, most of the numerical simulations of tunnel excavation are performed with linear-elastic perfectly-plastic models. Only a few studies on the influence of the nonlinear ground behaviour on calculated settlements above tunnels are at disposal (Gunn, 1993; Stallebrass et al, 1994; Addenbrooke et al., 1997).

Table 1. Parameters of the constitutive models

Model	E_0 MPa	p_0 kPa	α	ν	φ_p [°]	c_p kPa	φ_{cr} [°]	c_{cr} kPa	ψ [°]	κ	γ Mgm^{-3}
intact	200	-	-	0.27	36.5	50	-	-	0	-	2.57
1	44.6	-	-	0.37	32.9	8	-	-	21	-	2.37
2	31	200	0.6	0.37	32.9	8	-	-	21	-	2.37
3	31	200	0.6	0.37	32.9	8	28.6	15.5	21	0.21	2.37
4	-	200	0.6	0.37	32.9	8	28.6	15.5	21	0.21	2.37
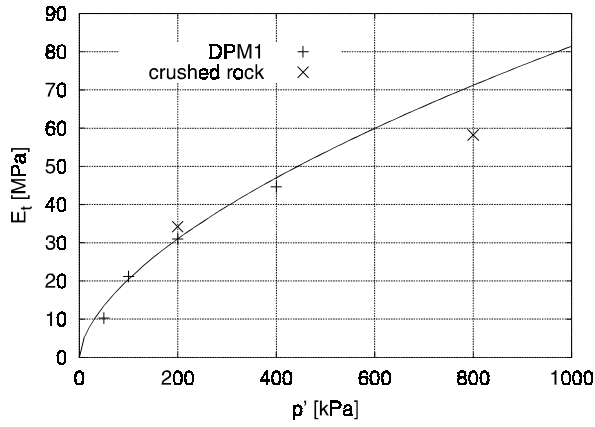
Figure 8. Calibration of E_0 and α.

Figure 9. Comparison of constitutive models 1 and 2 at two different stress levels.

In this paper, the intact rock mass was simulated by the isotropic linear-elastic perfectly-plastic (Mohr-Coulomb) model in the framework of small strains. Additionally, several material models were tested for the ground material in the weak zones with the parameters according to Table 1. A hierarchical development of the models was assumed, i.e., only one model property was changed for each enhancement.

2.1.1 *Model 1*

The linear-elastic perfectly-plastic model was assumed as a reference one. It considers the following ground parameters: elasticity modulus E_0, Poisson ratio ν, peak friction angle φ_p, peak cohesion c_p and dilatancy angle ψ.

2.1.2 *Model 2*

The stress-dependence of the elasticity modulus was included through the relationship
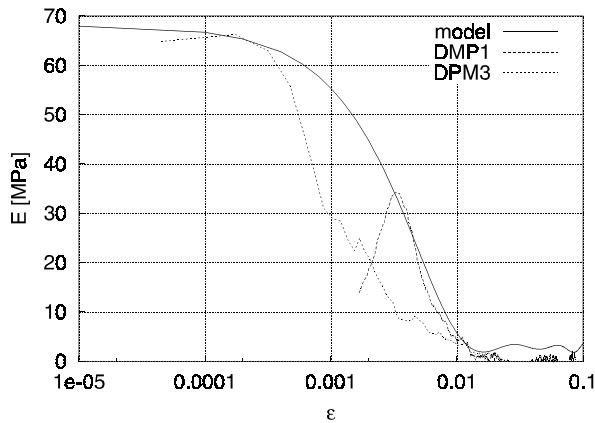
$$E = E_0 \left(\frac{p'}{p_0} \right)^\alpha . \tag{1}$$

The calibration of E_0 and α is in Figure 8 (the value of the reference pressure p_0 was chosen to be $p_0 = 200$ kPa). Figure 9 shows stress-strain curves from the numerical simulations of plane-strain compression tests at two different stress levels. A realistic increase of the stiffness with rising pressure can be observed for Model 2.

2.1.3 *Model 3*

Further improvement of the modelled ground behaviour was achieved by taking into account the softening of the stress-strain curve. Peak friction angle φ_p and cohesion c_p decrease to the critical state values φ_{cr} and c_{cr} after a prescribed amount of the plastic strain $\kappa = \sqrt{(0.5\varepsilon_{ij}^p \varepsilon_{ij}^p)}$. The rate of softening was estimated from standard triaxial compression tests. Nevertheless, this phenomenon has probably only a marginal effect on the calculated results since the limit stress condition is reached only in a small area around the tunnel (Figure 16).

2.1.4 *Model 4*

The final enhancement of the model (Model 4) includes a strain-dependent stiffness using the formulation (similarly to Gunn, 1993)

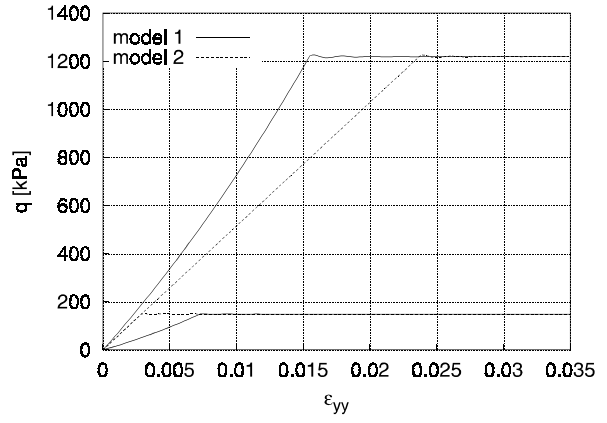Figure 10. Calibration of E_i, E_1, E_2..., E_8 from the outputs of triaxial tests.
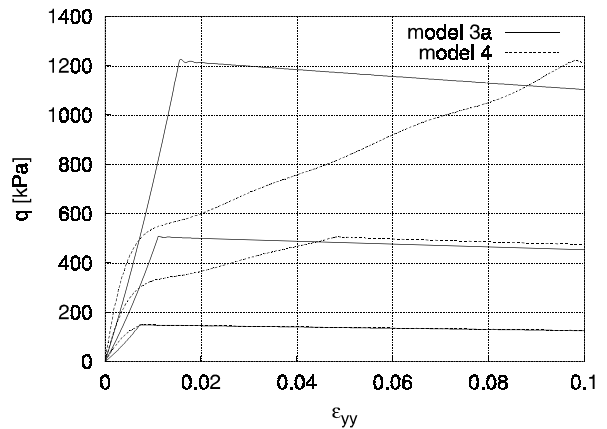

Figure 11. Comparison of constitutive models 3 and 4 at two different stress levels.
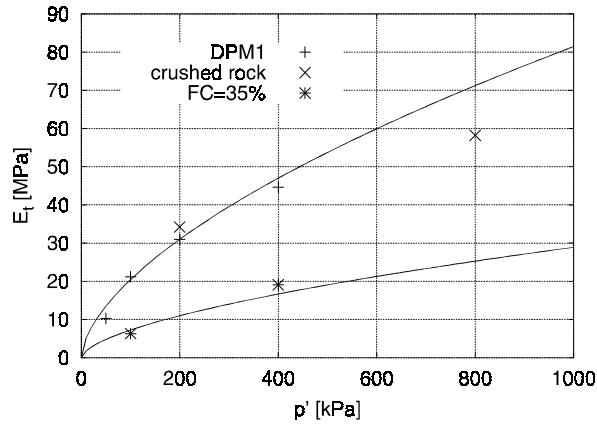
Figure 12. Calibration of E_0 and α for various materials from the weak zones.

Figure 13. FE mesh.

$$E_0 = E_i + E_1 \varepsilon^1 + E_2 \varepsilon^2 + \ldots + E_8 \varepsilon^8 \qquad (2)$$

for E_0 in Eq. (1) with

$$\varepsilon = \sqrt{\varepsilon_{ij}^* \varepsilon_{ij}^*} \qquad (3)$$

being the Euclidean norm of the deviatoric strain tensor. The parameters E_1, E_2,...,E_8 were obtained by curve fitting of the results from triaxial tests with both externally and locally measured axial deformation (Figure 10). Undesired oscillations resulting from the polynomial formulation of E_0 can be observed in the model curve for strains higher than 0.02. Nevertheless, these oscillations have only minor influence on the calculated stress-strain curves and, moreover, the level of strains in the analysed problem remains generally low (Figure 16).

A comparison of the stress-strain curves calculated with Models 3 and 4 is in Figure 11. The shape of the stress-strain curves produced by Model 4 is still not in a full agreement with experiments. Nevertheless, the improvement against Model 3 is obvious.

The outlined approach is certainly a very simple one. Several other approximations for the decay of E with strain have been proposed (e.g., Jardine et al,
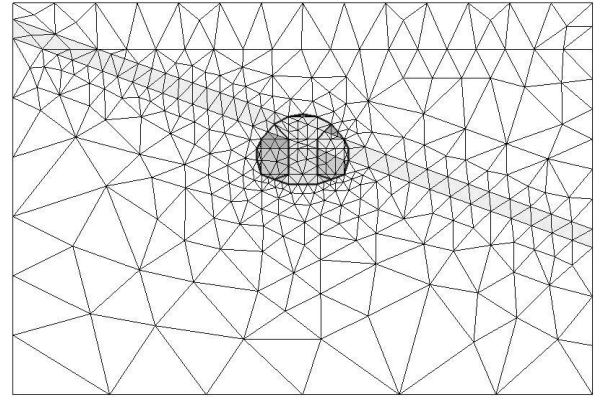
1986; Bolton et al, 1994; Atkinson, 2000). However, such models neglect anisotropy, loading direction and reversals, shear-volumetric coupling etc. A qualitatively better level can be reached by using elasto-plastic models with kinematic hardening or hypoplastic models which take into account the recent deformation history and strain direction (e.g., Stallebrass and Taylor, 1997; Niemunis and Herle, 1997). On the other hand, more sophisticated models require a significantly larger effort for their calibration and numerical implementation.

The material models and their parameters summarized in Table 1 are based on experimental results obtained for the sample DPM1 from one of the weak zones. However, a pronounced variability of the ground conditions in tectonic faults can be observed at the site of the Mrázovka tunnel. Therefore, further sets of ground parameters were determined from laboratory experiments (Table 2). Only Model 3 was considered since not enough tests with small strain measurements were available. The calibration of the parameters E_0 and α is shown in Figure 12.

All calculations were performed with the FE code Tochnog (Roddeman, 2001). This open source code enables modifications, and implementation of user-defined material models. The mesh consisted of

Table 2. Parameters of the material in the weak zones.

Material	E_0 MPa	p_0 kPa	α	ν	φ_p [°]	c_p kPa	φ_{cr} [°]	c_{cr} kPa	ψ [°]	κ
DPM1	31	200	0.6	0.27	34	0	30.5	0	21	0.21
crushed rock	31	200	0.6	0.27	45.1	0	38.3	0	21	0.21
FC 35%	11	200	0.6	0.27	31.7	0	28.3	0	21	0.21

Figure 14. Influence of the material model on the calculated surface settlement.
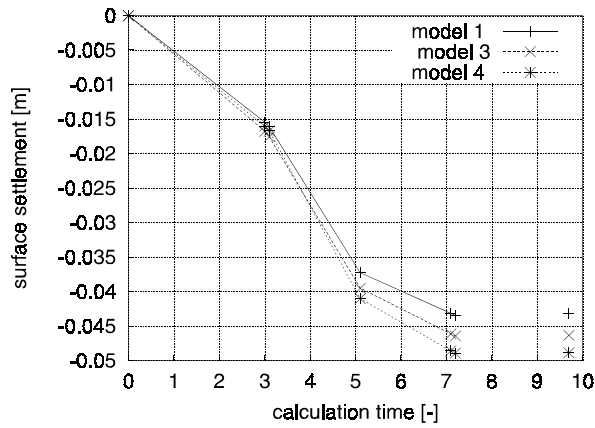

Figure 15. Influence of the material model on the calculated settlement of the crown.

680 constant strain triangular elements. Plane strain condition was assumed and horizontal displacements at the lateral boundaries and vertical displacements at the bottom were not allowed. The mesh is depicted in Figure 13. The tunnel is approximately 20 m below the ground surface, it is 12 m high and 16 m wide and the weak zone has the thickness of 3 m.

Initial stress conditions were geostatic. This implies an increase of the initial stiffness with depth for Models 2, 3 and 4. All stresses were effective since there was no water considered in the computational model. Implicit time integration was performed and inertia effects were not included.

The tunnel excavation was simulated by removing soil elements inside the tunnel and replacing them with equivalent nodal forces. These nodal forces at the tunnel boundary were subsequently partially reduced during several calculation steps. The applied "release factor" was 0.45. Finally, a concrete lining consisting of beam elements was installed. A staged excavation sequence was simulated as well.
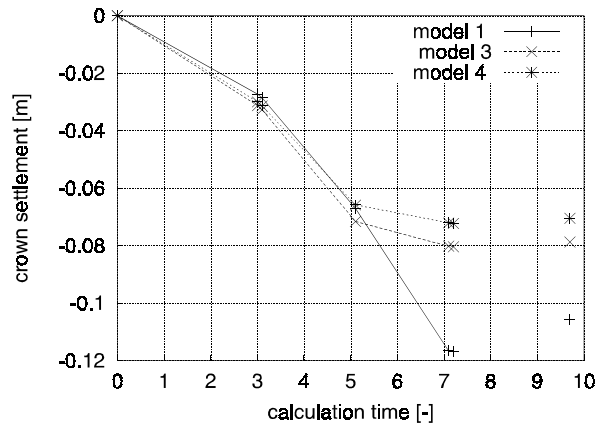
3 CALCULATION RESULTS

There is some influence of the material model on the maximum calculated settlement at the surface, see

Figure 14, although the difference may seem smaller than expected. The linear elastic Model 1 predicts the smallest surface settlement whereas the stress- and strain-dependent stiffness yields about 10% higher values. It should be reminded that the "intact" rock mass was modelled with a linear elastic model and the enhanced constitutive model was applied only in the weak zone. It can be expected that a strain-dependent stiffness of the entire ground would produce larger differences.

Much larger settlement differences due to the applied material models are obtained at the tunnel crown (Figure 15), which is located in the weak zone. The settlement of the crown predicted by Model 4 is by more than 50% larger than the deformation in linear elastic ground (Model 1). A slight decrease of the crown settlement at the final stage is due to the elastic heave of the ground produced by the excavation of the tunnel invert.

The distribution of the plastic strains is depicted in Figure 16. They are concentrated mainly in the weak zone close to the tunnel. The magnitude of plastic strains remains rather low which explains the negligible effect of the post-peak softening on the calculation results.

The role of the ground parameters (Model 3) and the excavation sequence can be observed in Figure 17.

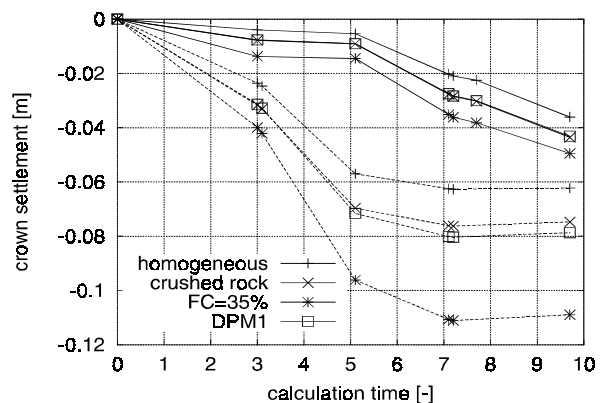Figure 16. Distribution of the plastic strains (darker regions) for Model 4.

Figure 17. Influence of the ground parameters and the excavation sequence on the calculated settlement of the crown (full line: vertical, dashed: horizontal sequencing).

The crown settlement may be doubled when the tunnel intersects a weak zone of a high clay content and thus of a low stiffness (horizontal sequencing, i.e., top heading and bench excavation). On the other hand, even a dramatic increase of the friction angle (cf. DPM1 and crushed rock) does not substantially diminish the deformations.

4 COMPARISON WITH MEASURED VALUES

A dramatic effect of the excavation sequence on the tunnel deformation is known. It was confirmed at the Mrázovka site. During the first 120 metres of excavation, vertical settlements of the overburden reached up to 209 mm, while the design limiting value was 60 mm. Such excessive deformations on excavating by horizontal sequencing indicated a danger of failure (Eisenstein et al, 2000) and forced the contractor to switch to the side drift method (vertical sequencing with side wall partial drifts followed by top heading and invert excavation).

The calculation results in Figure 17 suggest that in the weak zone with filling of higher FC (35%) the crown settlements can be reduced by more than 50% if the excavations sequence is changed. This is in accordance with numerical analyses by Barták et al (2000), who suggested that adopting the vertical sequencing should limit the vertical deformations at the surface by about 35%.

In further construction, the change of excavation sequence was accompanied with other ground control measures, such as grouting and forepoling by the Bodex technique. Therefore the maximum measured settlement of the surface was up to only 55 mm (Eisenstein et al, 2000).

5 CONCLUSIONS

For critical state strength, the tests on mixtures of coarse-grained and fine-grained fractions confirmed the existence of a distinct transition zone with respect to the content of fines. For the tested angular material the transition zone is in the interval of the fines content FC of 15% to 35%.

The decay of the parameters that depend on the soil structure, such as the peak strength or stiffness, starts at very small FC, and the behaviour does not comply with the simple structural concept. Further, the process does not have to be continuous, as was demonstrated for Young's modulus.

It has been concluded that the presence of fines in the coarse-grains' contacts, even at small FCs below the transition threshold, was responsible for the observed behaviour. Only after substantial strains, on the verge of the critical state, the fine-grained particles are forced to move from the contacts into the pores of the coarse-grained skeleton.

The strength of the fillings can be tested on specimens without the coarse fraction over 4 millimetres even for low FC. The comparison of data from a large cross-section shear box and standard 38 mm diameter triaxial apparatus showed that the strength of the specimens did not change, provided FCs of the samples were kept identical.

Numerical modelling showed that for the present problem deformation parameters were more important than the strength characteristics. Modelling of post peak softening did not change the results significantly and even the dramatic increase of the friction angle from 34° to 45° could not diminish deformations.

Deformations of the tunnel and its overburden were studied using three material models: with E constant, E dependent on stress and E dependent on stress and strain. The influence of the material model on surface settlement was rather small, about 10 %, since the enhanced model was used only for joints, while rock mass was modelled as linear - elastic.

The model with stress and strain dependent stiffness yielded by about 50 % larger deformation of the crown in comparison with the linear elastic model.

A dramatic influence of particle size distribution of the filling of the tectonic joint has been demonstrated. Predicted crown settlement for filling of FC above the transition zone was by about 50% larger than for material with low percentage of fines.

REFERENCES

Addenbrooke, T., Potts, D. and Puzrin, A. 1997. The influence of pre-failure soil stiffness on the numerical analysis of tunnel construction. *Géotechnique*, 47 (3): 693-71.

Atkinson, J. 2000. Non-linear soil stiffness in routine design. *Géotechnique*, 50(5): 487-508.

Barták, J., Hilar, M. and Chmelař, R. 2001. Model analysis of excessive deformations of the Mrázovka tunnel at the Northern front area (in Czech). *Zakládání staveb*, ISSN 1212-1711, Vol 13, No 1, 22-28.

Bolton, M., Dasari, G. and and Britto, G. 1994. Putting small strain non-linearity into Modified Cam Clay model. In Siriwardane and Zaman, editors, *Computer Methods and Advances in Geomechanics*, Balkema, 537-542.

Chmelař, R. and Vorel, J. 2000. Problems of the assessment of the rock massif in the NATM tunnelling of the Mrázovka Tunnel (in Czech). *Proc. Int. Conf. "Underground Construction"*, Prague, Czech Tun. Comm. ITA, 420-426.

Eisenstein, Z., Salač, M., Škrábek, J. and Zapletal, A. 2000. Mrázovka tunnel - prognosis, construction, reality (in Czech). *Proc. Int. Conf. "Underground Construction"*, Prague, Czech Tun. Comm. ITA, 465-476.

Gunn, M. 1993. The prediction of surface settlement profiles due to tunnelling. In: *Predictive soil mechanics* - Proc. Wroth memorial symposium, T.Telford, 304-316.

Jardine, R. J., Potts, D. M., Fourie, A. B. and Burland, J. B. 1986. Studies of the influence of non-linear stress-strain characteristics in soil-structure interaction. *Géotechnique*, 36(3): 377-396.

Mair, R. Taylor, R. and Bracegirdle, A. 1993. Subsurface settlement profiles above tunnels in clays. *Géotechnique*, 43(2): 315-320.

Mašín, D. 2001. The influence of filling of tectonic joints on tunnel deformations (in Czech). *MSc Thesis, Charles University*, Prague, 102 pp.

Niemunis, A. and Herle, I. 1997. Hypoplastic model for cohesionless soils with elastic strain range. *Mechanics of Cohesive-Frictional Materials*, 2(4): 279-299.

Roddeman, D. 2001. TOCHNOG: A free explicit/implicit FE program. http://tochnog.sourceforge.net/.

Stallebrass, S., Jovicic, V. and Taylor, R. 1994. Short term and long term settlements around a tunnel in stiff clay. In: I. Smith, editor, *Numerical Methods in Geotechnical Engineering*, Balkema, 235-240.

Stallebrass, S, and Taylor, R. 1997. The development and evaluation of a constitutive model for the prediction of ground movements in overconsolidated clay. *Géotechnique*, 47(2): 235-253.

Thevanayagam, S. and Mohan, S. 2000. Intergranular state variables and stress-strain behaviour of silty sands. *Géotechnique*, 50 (1), 1-23.